Extended liquid-crystalline oligofluorenes with photo- and electroluminescence

Jesús del Barrio,[a] Luiz Silvino Chinelatto Jr.,[a] José Luis Serrano,[b] Luis Oriol,*[a] Milagros Piñol*[a] and Henk J. Bolink[c]

Received (in Montpellier, France) 28th May 2010, Accepted 14th July 2010
DOI: 10.1039/c0nj00404a

In this paper we report the synthesis and characterization of a series of low-molecular weight light-emitting molecules based on short oligofluorene cores, from one to three 9,9-dioctylfluorene units, elongated at the 2- and 7-positions by means of promesogenic units. The effect of this structural modification on the mesomorphic properties, as well as on the optical and electrochemical properties, is studied. The possibility of using these molecules as emitters in light-emitting diodes (LEDs) and polarized photoluminescent layers has been explored.

Introduction

Amongst linearly π-conjugated purely organic systems, polyfluorenes and related oligomers have been much investigated as photo- and electro-stimulated emissive materials for flat-panel display applications. This relies on the fact that they combine an almost unique set of chemical, thermal, optical, and electronic features that can be easily tailored through molecular design. From a structural point of view, polyfluorenes with extended π-conjugation and a stiff backbone are ideal luminescent materials due to their high efficiency and good thermal stability but also for their potential liquid crystalline properties. In fact, many systematic structure–activity reports showing the versatility of polyfluorenes can be found in the literature.[1–5]

Polymers have the advantage of high T_g and good film forming ability but also drawbacks concerning their high viscosity and limited solubility. In this sense, oligofluorenes with well-defined chain lengths and end groups represent an unquestionable alternative to their polymer counterparts.[6–8] In contrast to polymers, monodispersed oligomers are characterized by structural uniformity and regularity that generally turns into more predictable and reproducible properties that can also be optimized more easily.[9] However, the synthesis of monodisperse oligomers involves a large number of steps and lengthy purification procedures, and has proven to be difficult in most cases.

The photoluminescent properties of a large number of polyfluorenes and oligofluorenes have been described; in particular, a large number of reports concern their use to polarize the emission.[6,10–14] When their intrinsic structural anisotropy is combined with liquid-crystalline behavior, these systems can be spontaneously oriented and macroscopically aligned by surface forces, giving rise to optical anisotropies and a linearly polarized luminescence. Electroluminescence has also been extensively investigated. For electroluminescence, a balanced charge injection of holes and electrons in the luminescent material is crucial to achieve a high device performance; therefore, materials with low ionization potential (IP) and high electron affinity (EA) are required. In general, most organic materials used as emitters for electroluminescence inject and transport holes more efficiently than electrons due to their richness of π-electrons. The liquid-crystalline, electronic and optical properties of fluorene-based oligomers are primarily governed by the chemical structure of the backbone, *i.e.* the size of the π-core, the type and number of side chains, or incorporation of terminal chains and/or functional groups.[15–17] For instance, the absorption and emission wavelengths are determined by the energy of the optical band gap (ΔE_{gap}). However, the injection of electrons and holes is controlled by the HOMO (or ionization potential) and LUMO (or electron affinity) levels. From the synthetic point of view, a standard strategy to modify the optoelectronic properties of a molecule is to include electron-withdrawing or electron-donating groups in its aromatic core; thus, it is possible to tune the HOMO and LUMO energy levels and alter their electronic properties by choosing suitable functional groups.[18]

From the point of view of the chemical structure, when compared to the π-isoelectronic biphenyl unit, the fluorene ring has a more planar and rigid structure with a lower level of conformational freedom because of the presence of the methylene bridge. This structural feature gives a red-shift in the emission and improves the emission efficiency. However, because the fluorene unit is slightly bent, the non-coaxial structure of the 2,7-disubstituted fluorene core has an adverse effect on the liquid-crystal properties. In addition, the usual presence of alkyl chains or bulky side groups at the bridging 9-position of the fluorene units to increase the solubility in organic solvents and to limit the formation of aggregates in the solid state, lowers the melting point and imparts a high tendency for glass formation.[19] The adverse effect is that substitution at the bridging methylene gives rise to larger intermolecular distances, hindering the molecular packing required for the development of liquid-crystallinity in short

[a] *Química Orgánica, Facultad de Ciencias-Instituto de Ciencia de Materiales de Aragón, Universidad de Zaragoza-CSIC, 50009-Zaragoza, Spain. E-mail: loriol@unizar.es, mpinol@unizar.es; Fax: +34 976 761209; Tel: +34 976 762279*
[b] *Química Orgánica, Facultad de Ciencias-Instituto de Nanociencia de Aragón, Universidad de Zaragoza-CSIC, 50009-Zaragoza, Spain*
[c] *Instituto de Ciencia Molecular, Universidad de Valencia, P.O. Box 22085, Valencia, Spain*

oligomers (in general, from dimers to pentamers) with low length-to-breadth ratios.[7,20] Moreover, structural changes of the (phenylethenyl)fluorene have shown that large alkyl chains can preclude either crystallization or the formation of a glassy state at room temperature, providing fluid oils, which can act to the detriment of the morphological stability of electroluminescent devices.[21]

There are examples of liquid-crystalline fluorene analogues of biphenyl with nematic and smectic mesophases over narrow temperature ranges.[22,23] Elongation of the π-system of one fluorene core just by one or two additional 4-substituted phenyl rings is enough to promote liquid-crystallinity, mainly smectic phases, so long as the fluorene is not substituted at the bridging 9-position or has appended short alkyl chains.[24–27] Otherwise, if larger alkyl pendant chains are desired to suppress crystallization and to lower the melting point, the number of aromatic rings has to increase; this strategy has been pursued in the literature to design a fluorene-based liquid-crystal with luminescent or electronic charge transport properties, which also have terminal alkyl chains in some cases with reactive groups in order to provide liquid-crystalline networks.[15,19,28]

Systematic studies of oligofluorenes have also been undertaken and luminescent liquid-crystals have been described consisting of three fluorene units with a methyl group and flexible terminal chains showing smectic and nematic phases at temperatures above 100 °C. If 4 or 5 fluorene units with longer aliphatic lateral chains are required, synthesis becomes exponentially more difficult.[6]

Here, we report the synthesis and properties of a series of novel molecules mainly based on two 9,9-dioctylfluorene units whose rigid core has been extended with well-known 4-cyanophenyl or 4-cyanobiphenyl termini, or even phenyl ester pro-mesogenic segments. From a structural point of view, we are particularly interested on having long lateral chains to promote glassy states and on the incorporation of the 4-cyanophenyl terminal fragments to tailor liquid-crystallinity, photoluminescence and electroluminescence because its strong withdrawing character to enhance electron transporting properties[29] and its proclivity to promote the Nematic liquid-crystalline phase, which is the preferred over the Smectic phases because of its lower viscosity when processing films is required.[19] We report a detailed optical and electrochemical characterization of these fluorene-based luminophores and some preliminary work that shows how they can be used for electroluminescent devices and polarized photoluminescent layers.

Results and discussion

Synthesis and structural characterization of the oligofluorenes

Scheme 1 shows the structure of the target oligofluorenes and the corresponding synthetic pathways. The oligofluorene-based cores were built up by aryl–aryl Suzuki coupling reaction between aryl halides and arylboronic acids or arylboronates as reported for related oligofluorenes.[6,30] The reactions were conducted using tetrakis(triphenylphosphine)-palladium(0) as the catalyst, and sodium carbonate as the base in dimethoxyethane at 75 °C or toluene at 90 °C depending on the solubility of the required boronic acids; the reaction was initially conducted in toluene but due to the lack of solubility of some boronic derivatives (in particular, boronic acids **3** and **4**), the more polar solvent dimethoxyethane was used. Conjugated cores containing two fluorene units, **CN-PFFP-CN**, **CN-PPFFPP-CN** and the intermediate **HO-PFFP-OH**, were obtained by coupling the dibromide fluorene (**2**) with different monoboronic derivatives (**3**, **4**, or **5**) in a ~1 : 2.1 molar ratio. The reaction of dibromide (**1**) in approximately equimolar proportion with boronic acid (**3**) gives rise to the dicoupled derivative with one fluorene unit **CN-PFP-CN** but also renders the monocupled product **CN-PF-Br**, which in turn reacts with the diboronate ester (**6**) to yield the oligofluorene homologue with three fluorene units, **CN-PFFFP-CN**. Finally, the last oligofluorene of this series, **C_5PPCOO-PFFP-OCOPPC_5**, was prepared by an esterification reaction of the intermediate **HO-PFFP-OH** with the acyl chloride of the 4′-pentylbiphenyl-4-carboxylic acid (**7**). Molecular structures were proved by spectroscopic techniques, IR and NMR, as well as MALDI spectrometry. Data are gathered in the Experimental section.

Thermal characterization of the oligofluorenes

Thermal stability was investigated by thermogravimetric analysis (TGA) under nitrogen atmosphere; the data is presented in Table 1. These oligofluorenes have good thermal stability, the onset temperature of the thermal degradation with associated mass loss being above 360 °C in all cases. It is clear that the elongation of the aromatic core induces a considerable increase in the stability of this series; therefore, when the structurally related homologues **CN-PFP-CN**, **CN-PFFP-CN** and **CN-PFFFP-CN** are compared the T_{onset} of the weight loss goes up from 361 °C to 418 °C and 425 °C, respectively.

Oligofluorenes were obtained as only partially crystalline solids at room temperature that, once melted, had low tendency towards crystallization. The absence of crystallization was proved by DSC where, after cooling the sample from the isotropic state at 10 °C/min, a 'jump' on the baseline of the subsequent heating curve corresponding to the T_g was detected in all cases (Fig. 1). Comparison of the **CN-PFP-CN**, **CN-PFFP-CN** and **CN-PFFFP-CN** data shows that T_g increases on increasing the length of the aromatic core. Together, the increase on the number of the aliphatic chains hinders the crystallization propensity. In this respect, the compound **CN-PFP-CN** displays a cold crystallization process above the T_g and a subsequent endothermic peak associated with melting of the just-formed crystalline phase. This situation is not reproduced with the higher homologues of the series, which remain as amorphous solids.

When inspected under the polarizing optical microscope (POM), compounds **CN-PPFFPP-CN** and **C_5PPCOO-PFFP-OCOPPC_5** are liquid-crystals. In both cases, well-defined *Schlieren* and *threaded-like* textures associated with the nematic phase are observed (see Fig. 2). The nature of the mesophase was also confirmed by X-ray diffraction. A detailed inspection of **CN-PPFFPP-CN** proves that it is a monotropic liquid-crystal, *i.e.* the mesophase only forms on cooling the

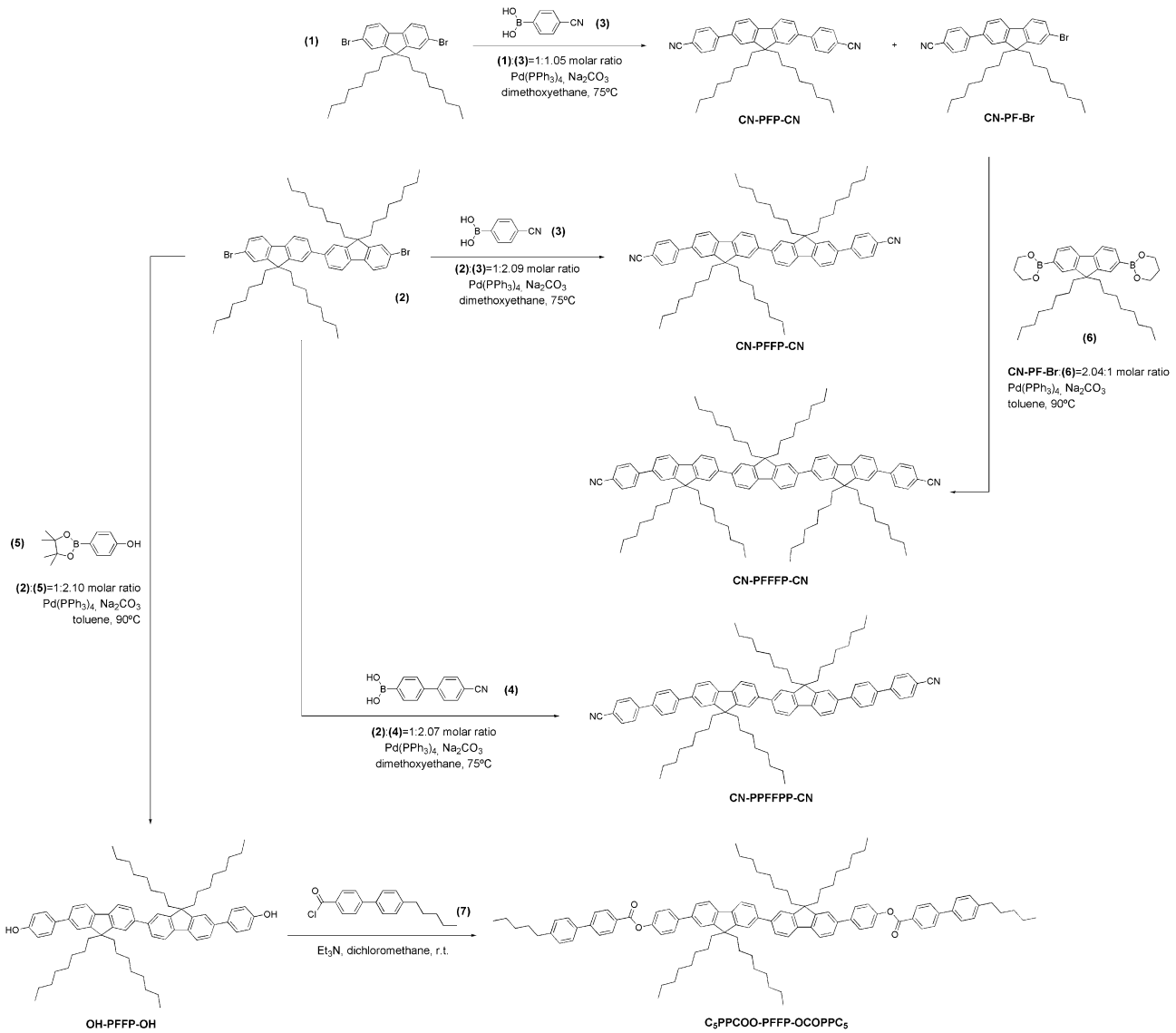

Scheme 1

Table 1 Thermal and thermodynamic data for the oligofluorenes

	TGA[a]		Transition temperatures and enthalpies[b]												
Compound	T_{onset}	DTGA	1st heating[c]						2nd heating[d]						
CN-PFP-CN	361	391	C	108 (28.2)	I				g	15	[77 (−15.6)	C	106 (17.0)]	I	
CN-PFFP-CN	418	447, 488, 525	C	130 (34.8)	I				g	17	I				
CN-PFFFP-CN	425	450, 581	C	85 (37.6)	I				g	26	I				
CN-PPFFPP-CN	418	451, 582	C	117 (9.77)	I				g	32	N		105 (—)	I	
C_5PPCOO-PFFP-OCOPPC_5	424	451, 533	C	142 (36.6)	N	255 (—)	I		g	29	N		250 (1.0)	I	

[a] Thermogravimetry analysis. T_{onset}: Decomposition temperature given in °C at the onset of the weight loss curve; DTGA: first derivative of the weight loss curve. [b] g: glass; C: crystal; I: isotropic liquid; N: nematic. Temperatures are given in °C, values in brackets correspond to enthalpy transitions given in kJ/mol. [c] Heating rate 10 °C/min. [d] Heating rate 20 °C/min.

isotropic liquid. Interestingly, because of the resistance to crystallization, the nematic phase vitrifies on cooling below the T_g, giving a mesomorphic glass, for which it is possible to observe the mesophase on heating between T_g = 32 °C and $T_i \approx$ 105 °C. The glass crystallizes on standing above T_g. For **C_5PPCOO-PFFP-OCOPPC_5** the incorporation of the promesogenic 4′-pentylbiphenyl unit by an ester linkage instead of a nitrile end group stabilizes the mesophase that appears on heating in a wide temperature interval.

Following these observations, we can infer that the π-elongation of the aromatic core with the 4-cyanophenyl end group has not been successful up to the terfluorene core.

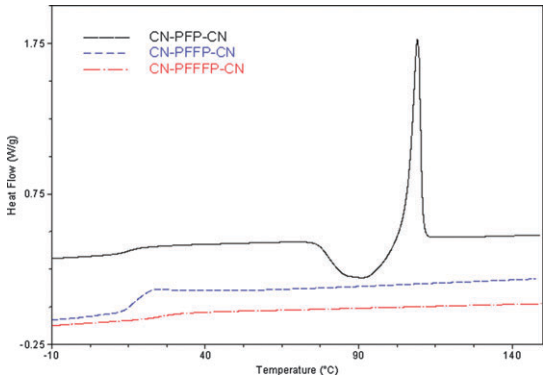

Fig. 1 DSC curves recorded at 20 °C/min after previous controlled heating and cooling scans at 10 °C/min.

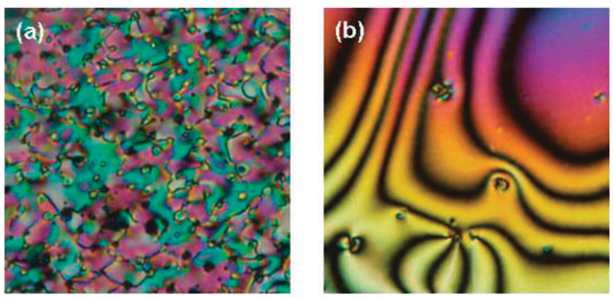

Fig. 2 Microphotographs of the nematic phase of the (a) threaded-like texture observed for **CN-PPFFPP-CN** developed on cooling at 80 °C, and (b) the Schlieren texture observed for **C_5PPCOO-PFFP-OCOPPC_5** developed on cooling at 30 °C.

However, elongation of the bifluorene with promesogenic units 4-cyanobiphenyl or phenyl 4′-pentylbiphenyl-4-carboxylate is a much better alternative in order to induce liquid-crystallinity.

Compounds **CN-PFFFP-CN** and **CN-PPFFPP-CN** are π-isoelectronic; they both have eight aromatic rings and terminal nitrile groups but they differ in the number of fluorene units. Their differences in the mesomorphic properties can be related to the fact that **CN-PFFFP-CN** has two additional bulky *n*-octyl lateral chains that decrease the length/diameter ratio and hinder mesomorphism.

Electronic and electrochemical properties in solution

When considering applications in organic devices, evaluation of the electronic and electrochemical properties is required. The properties have been studied by UV-vis and fluorescence spectroscopies and cyclic voltammetry.

Absorption and emission spectra of the compounds were recorded in THF solution, and representative data are collected in Table 2. All the compounds show unstructured absorption bands located at 342–372 nm due to π–π* transitions, and an efficient emission in the violet-blue region. In particular, the emission quantum yield values of the nitrile derivatives, $\phi_{em} \approx 0.7$–0.8, are comparable to the value reported for the poly(9,9-dioctylfluorene), $\phi_{em} \approx 0.8$.[30] As it was expected, increasing the conjugation length on moving from **CN-PFP-CN** to **CN-PFFP-CN** and **CN-PFFFP-CN** gives a bathochromic shift on both absorption and emission

Table 2 Optical properties of the oligofluorenes in THF[a]

Compound	λ_{abs} (log ε)	ΔE_{gap}[b]	λ_{em}[c]	ϕ_{em}
CN-PFP-CN	342 (4.80)	3.28	386	0.69
CN-PFFP-CN	362 (4.95)	3.08	412, 428	0.76
CN-PFFFP-CN	372 (5.01)	3.02	417, 438	0.78
CN-PPFFPP-CN	364 (5.02)	3.07	417, 438	0.79
C_5PPCOO-PFFP-OCOPPC_5	352 (4.99)	3.20	396, 416	0.61

[a] λ in nm, ε in M^{-1} cm^{-1}, Δ*E* in eV. [b] Optical band gap calculated as $\Delta E_{gap} = 1240/\lambda_{onset}$, where λ_{onset} is the low-energy absorption edge in THF solution. [c] Maximum wavelength of the emission registered when excitation at λ_{abs}.

maxima together with an increase on the emission efficiency. The optical band gap, ΔE_{gap}, considered as the HOMO–LUMO separation, was estimated from λ_{onset} of the low absorption band, which for this series of compounds varied from 3.28 to 3.02 eV with the value decreasing on increasing the number of fluorene units on the aromatic core. This predictable trend can be related to the narrowing of the HOMO–LUMO gap on increasing the effective conjugation length.

On comparing **CN-PFFFP-CN** and **CN-PPFFPP-CN**, which have aromatic cores of the same-length, a hypsochromic shift can be observed in both the absorption and emission bands, together with increase of ΔE_{gap} for the latter. This is associated with the more planar and rigid structure of the fluorene unit with a lower level of conformational freedom than the π-isoelectronic biphenyl unit.

We should also emphasise the optical properties of **C_5PPCOO-PFFP-OCOPPC_5** when compared to the nitrile-terminated homologous **CN-PFFP-CN**, which has the same aromatic core. A hypsochromic shift on both absorption and emission was observed, together with a smaller optical band gap for **C_5PPCOO-PFFP-OCOPPC_5**. These differences are ascribed to the moderate electron-donating character of the terminal –OCOPPC_5 ester group in comparison to the electron-withdrawing character of the –CN group. Also, the presence of terminal –CN groups allows better emission yields than ester groups.

Cyclic voltammetry (CV) studies were carried out to investigate the redox properties in solution, and relevant data is collected in Table 3. Under our experimental conditions, reduction features were not observed at potentials from 0 to −2 V. However, one or two reversible/quasi-reversible oxidation waves – yielding, sequentially, monoradical cation and dication species – were registered for all the compounds. The chain-length dependence of the oxidation potentials fits with the behavior of monodisperse oligofluorenes with pendant 2-ethylhexyl chains in the C9 position described by Chi *et al.*[31] As we compare the data obtained by CV, it shows that increasing the number of fluorene units leads to an increase of the accessible oxidation states in related compounds, from one in **CN-PFP-CN**, to two in **CN-PFFP-CN** and **CN-PFFFP-CN** (see Fig. 3). In the last-mentioned compound, the two oxidation couples can be clearly differentiated. A negative shift of the half-wave oxidation potentials and a decrease of the difference between successive half-wave potentials (*i.e.*, $E^2_{1/2} - E^1_{1/2}$) are also observed on increasing the number

Table 3 Cyclic voltammetry data in solution[a] and energy level analysis[b] of the oligofluorenes

Compound	$E^1_{1/2}$ (V)	$E^2_{1/2}$ (V)	E_{onset} (V)	HOMO (eV)	LUMO (eV)
CN-PFP-CN	1.63[qr]	—	1.55	−5.95	−2.67
CN-PFFP-CN	1.38	1.74[qr]	1.32	−5.77	−2.69
CN-PFFFP-CN	1.27	1.49	1.21	−5.61	−2.59
CN-PPFFPP-CN	1.30	1.56[qr]	1.24	−5.64	−2.57
C_5PPCOO-PFFP-OCOPPC$_5$	1.56	1.77[qr]	1.50	−5.90	−2.70

[a] $E_{1/2}$: half-wave potential calculated as the midpoint between the cathodic and anodic peaks. $E^1_{1/2}$: corresponds to the first oxidation couple and $E^2_{1/2}$: corresponds to the second oxidation couple. For quasi-reversible (qr) processes the values is only an estimate. E_{onset}: onset potential for the first oxidation wave. [b] HOMO and LUMO energy level values are given relative to the vacuum level. The HOMO was calculated from the oxidation potentials assuming the energy level of Ag/AgCl to be 4.4 eV below the vacuum level. The LUMO was calculated from the optical band gap.

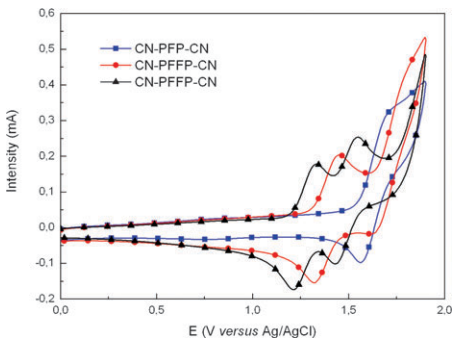

Fig. 3 Cyclic voltametry curves of 4-cyanophenyl-terminated oligofluorenes in dichloromethane.

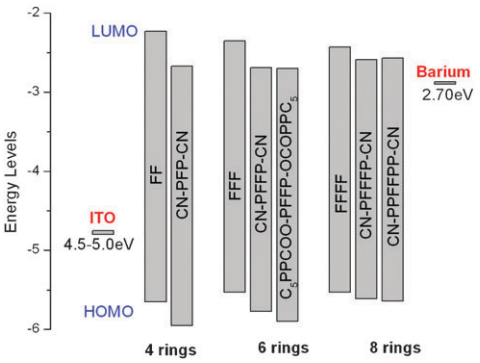

Fig. 4 HOMO–LUMO values depicted as the energy to the vacuum level for the extended oligofluorenes compared to oligofluorenes having the same number of aromatic rings.

of fluorene units, which can be related to the increase of the π-conjugation length.

On the other hand, by comparing data obtained for compounds **CN-PFFFP-CN** and **CN-PPFFPP-CN** it can be observed that, in spite of being π-isoelectronic, the oxidation potentials shift towards more positive values and also the difference between successive half-potentials increases for **CN-PPFFPP-CN**. The differences might be related to the larger planarity of the aromatic core in **CN-PFFFP-CN**, which provides a larger effective conjugation length, in agreement with optical measurements.

The HOMO and LUMO energy levels referred to the vacuum level have been estimated by combining electrochemical and optical data, and values are summarized in Table 3 and depicted in Fig. 4. Obtaining absolute HOMO and LUMO levels in this way is an issue in debate, but in this case the values obtained are considered to provide a rough approximation.[32] Therefore, HOMO was determined from the oxidation potential by the empirical relationship: HOMO = $-(E_{onset} + 4.4)$ eV where E_{onset} is the onset potential for the first oxidation wave relative to the Ag/AgCl reference electrode.[29] The LUMO, which in our particular case could not be obtained by electrochemical measurements, was deduced from the optical band gap using the expression: LUMO = HOMO + ΔE_{gap}.

On the systematic extension of the aromatic core from **CN-PFP-CN** to **CN-PFFFP-CN**, the HOMO energy level rises from −5.95 eV to −5.61 eV. However, the LUMO levels are essentially comparable, ranging from −2.7 to −2.6 eV. The corresponding values estimated for the π-isolectronic **CN-PFFFP-CN** and **CN-PPFPP-CN** are essentially similar, with a slightly discernible lowering of the HOMO and increasing of the LUMO levels for the latter. Finally, for **C_5PPCOO-PFFP-OCOPPC$_5$** a larger stabilization of the HOMO level than of the LUMO was observed when values were compared to the nitrile-terminated homologous **CN-PFFP-CN**.

The HOMO and LUMO levels of 9,9-dioctyloligofluorenes (**FF**, **FFF** and **FFFF** according to our nomenclature) having the same overall number of aromatic rings (4, 6 or 8) within the core were also determined by combining CV and UV-vis data.[33] On comparing data for compounds having the same number of rings, *i.e.* **FF** *vs.* **CNPFPCN**, or **FFF** *vs.* **CNPFFPCN**, or **FFFF** *vs.* **CNPFFFPCN** and **CNPPFFPPCN**, we can infer that the HOMO and LUMO levels are slightly lower for the nitrile-terminated compounds than for the corresponding 9,9-dioctyloligofluorenes (see Fig. 4).

Electroluminescence properties

Double-layered devices with an ITO/PEDOT:PSS/oligofluorene/Ba/Ag configuration were fabricated to investigate the electroluminescent properties (see Table 4). The devices were prepared by spin-coating a PEDOT:PSS hole-transporting layer onto a glass substrate covered by an ITO anode. The light-emitting layer was spin-cast onto the PEDOT:PSS layer, and covered by a barium cathode. Silver was deposited on the top of the device to protect the barium electrode. For the light-emitting layer, **CNPFPCN**, **CNPFFPCN** and **CNPFFFPCN** were blended with inert PS at 50% weight. It has been described that handling solids is preferred to fluid oils in terms of device performance and also that blending with polymers

Table 4 Performance characteristics of ITO/PEDOT:PSS/oligofluorene/Ba/Ag electroluminescent devices[a]

Emitter	V_{on} (V)	Luminance (cd/m^2)	Current efficiency (cd/A)
CN-PFP-CN	7.5	10.2	0.08
CN-PFFP-CN	7.0	45.8	0.30
CN-PFFFP-CN	6.5	3.6	0.71

[a] V_{on}: turn-on-voltage, defined as the voltage required to reach 0.1 cd/m^2.

might reduce the undesired greenish emission in fluorenes.[21] Our target compounds have T_g values at approximately room temperature (15–26 °C); nevertheless, because the low T_g of the oligomers limits the formation of good films, the emitter was dispersed into inert PS to obtain good films that do not lead to a short-circuit upon depositing the metal counterelectrode.

The current–voltage–luminance (*I–V–L*) characteristics show that the devices have turn-on voltages of 7.5–6.5 V, with the turn-on voltage decreasing on decreasing the barrier for hole injection from the ITO electrode (see Fig. 4). As it would be expected, the luminophores with better photoluminescence quantum yields in solution have better current efficiency, as seen from the efficiency evolution in Fig. 5. A maximum luminance of 45.8 cd/m^2 at a current density 79.7 A/m^2 was achieved for the emitter **CN-PFFP-CN** with a turn-on voltage of 6.9 V.

Electroluminescence (EL) spectra were also recorded. In Fig. 6 the EL spectra of **CN-PFFFP-CN** is shown and compared to the photoluminescence (PL) in solution. The bathochromic shift and broadness of the emission band on the electroluminescence spectra when compared to the photoluminescence in solution is presumably due to a more planar excited state in the solid state. Nevertheless, it has also to be considered that the appearance of a long-wavelength emission in polyfluorenes could be associated with the formation of keto-defects at the fluorene bridge, which is related to the deterioration of device performance.[34] The CIE 1931 chromaticity coordinates of the device shown in Fig. 6 are $x = 0.20$ and $y = 0.24$.

Polarized emission from liquid-crystalline networks

The fluorene core exhibits direction-dependent absorption and emission, with the transition moment polarized along the longitudinal axis of the molecule. Therefore, polarized photoluminescent films can be produced if the sample is uniformly aligned in the liquid-crystal fluid state and the molecular alignment can preserved in the solid state. To evaluate the potential of these systems for polarized photoluminescence, macroscopically anisotropic films with a guest–host configuration were prepared by *in situ* photopolymerization of a host non-emissive reactive liquid-crystalline matrix containing fluorenes as an emissive guest (Table 5).

A liquid-crystal matrix consisting of monoacrylate and diacrylate liquid-crystals was doped with 5 mol% of the luminophore. The reactive mixtures were investigated by POM with appropriate light filters and DSC, and photopolymerization verified by photo-DSC. They developed a nematic phase between 65–60 °C and 120–140 °C, and were homogeneous under POM inspection. Once in the molten state, all of them showed a small tendency towards crystallization on cooling.

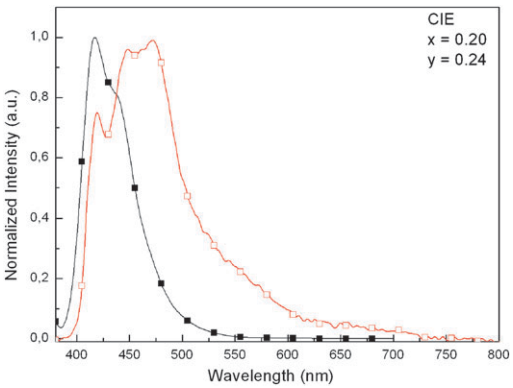

Fig. 6 Photoluminescence (solid symbols) in solution and electroluminescence (open symbols) spectra for **CN-PFFFP-CN**. The CIE chromaticity coordinates of the electroluminescent device are indicated.

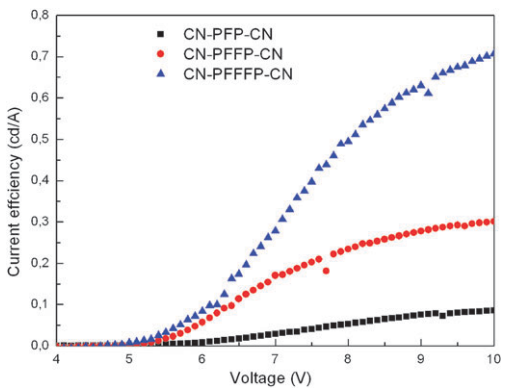

Fig. 5 Current efficiency *versus* applied voltage for the EL devices with a configuration ITO/PEDOT:PSS/oligofluorene/Ba/Ag.

Table 5 Thermal properties of the investigated reactive blends and emission properties of the anisotropic polymeric films

Luminophore	Thermal transitions[a]					λ_{em} (nm)[b]	R_{em}[b]
CN-PFP-CN	C	55	N	123	I	410	7
CN-PFFP-CN	C	60	N	120	I	430	6
CN-PFFFP-CN	C	54	N	119	I	440	5
CN-PPFFPP-CN	C	55	N	127	I	434	8
C_5PPCOO-PFFP-OCOPPC_5	C	55	N	140	I	420	8

[a] Data collected from DSC curves corresponding to the first heating scan at 10 °C/min rate. Transition temperatures given in °C: C: crystal; I: isotropic liquid; N: nematic. [b] Maximum wavelength of the emission and emission dichroic ratio (R_{em}) defined as the intensity ratio of the parallel and perpendicular polarization of the polymeric films ($I_{\parallel}/I_{\perp}$).

Anisotropic polymeric networks were produced by UV photopolymerization using commercial cells for planar alignment. To achieve maximum ordering, cells were filled by capillarity, heating the mixture into the isotropic liquid state, followed by slowly cooling into the nematic phase. In the course of the polymerization, transparent films with good optical quality and a single-domain structure with good planar orientation were obtained, as observed by POM. After testing several temperatures (room temperature, 60 and 80 °C), the blends were polymerized at 60 °C, because at this temperature films with the highest optical anisotropy were processed.

The emission spectra of the films show similar bands that are red-shifted when compared to those registered in diluted solution, presumably due to emission from a more planar structure in the solid state.[6] Polarized emission spectra were recorded both parallel to the rubbing direction in the cell and perpendicular to it using polarized excitation parallel to the rubbing orientation. Films exhibited direction-dependent emission, maximum in the preferential orientation direction in the cell ($I_{\parallel}$), and minimum perpendicular to it ($I_{\perp}$), which indicates that the oligofluorenes align parallel to the polarization direction of the incident UV beam.

The emission anisotropy ratio (R_{em}), defined as the quotient between these two values, depends on several factors. The polarization ratio depends on molecular aspects such as the angle of the absorption and emission transition moments to the long molecular axis, rotational diffusion, as well as macroscopic features such as the degree of order within the film. Nevertheless, for comparative purposes, in films of this series of structurally related fluorenes, R_{em} values can give some information about the orientation.

On comparing values obtained for **CN-PFP-CN**, **CN-PFFP-CN** and **CN-PFFFP-CN**, it can be inferred that, in spite of their lack of liquid-crystallinity, due to their rod-like shape these oligofluorenes are preferentially oriented within the liquid-crystal matrix. Nevertheless, the emission anisotropy lowers significantly on increasing the number of fluorene units from $R_{em} \approx 7$ for **CN-PFP-CN** to $R_{em} \approx 5$ for **CN-PFFFP-CN**. One should expect larger emission anisotropies on increasing the π-length but, in this case, the number of *n*-octyl chains increases from two to six, lowering the effective aspect ratio and likely impeding the uniaxial molecular orientation.

Accordingly, compound **CN-PPFFPP-CN** gives rise to emission anisotropy $R_{em} \approx 8$ compared to the mentioned value of $R_{em} \approx 5$ of the π-isoelectronic **CN-PFFFP-CN** (Fig. 7). This comparison underlines the adverse effect of the long *n*-octyl chains on the degree of alignment.[4] Nevertheless, it can not be underestimated that the liquid-crystalline properties of this compound can also favor the alignment within the liquid-crystalline matrix. In this sense, a comparable emission anisotropy value of $R_{em} \approx 8$ was determined for the liquid-crystal compound **C_5PPCOO-PFFP-OCOPPC_5**. Therefore, it is expected that both factors (*i.e.* low number of alkyl lateral chains and mesomorphism) contribute to achieve the largest degree of orientational order.

Finally, for the sake of comparison, oriented networks were also processed from oligofluorenes **FF**, **FFF** and **FFF** under the same experimental conditions. Anisotropy emission values of

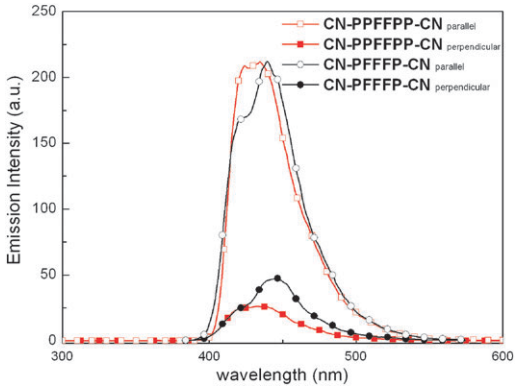

Fig. 7 Polarized photoluminescence spectra of films processed from **CN-PFFFP-CN** (circles) and **CN-PPFFPP-CN** (squares) taken parallel (open symbols) and perpendicular (solid symbols) to the preferred molecular orientation direction.

R_{em} = 1.7–2.0 were determined which are substantially lower than those obtained for the reported extended oligofluorenes with the same number of aromatic rings. To interpret these results, not only the effect of the core length and the number of the alkyl chains must be considered, but also the effect of the nitrile end groups on increasing the electronic polarizability of the molecule.

Experimental section

Materials synthesis

All chemicals and reagents were used as received from their commercial sources, except toluene, which was dried over sodium and distilled. Reactions were conducted under argon. 2,7-Dibromo-9,9-di(*n*-octyl)fluorene (**1**) was obtained from 2,7-dibromofluorene using 1-bromooctane, NaOH and tetra-(*n*-butyl)ammonium in 81% yield.[26] 2,7′-Dibromo-9,9,9′,9′-tetra(*n*-octyl)bifluorene (**2**) was obtained by bromination of 9,9,9′,9′-tetra(*n*-octyl)bifluorene using $Br_2/FeCl_3$ in 88% yield.[35] Boronic derivatives 4-cyanophenylboronic acid (**3**), 4′-cyanobiphenyl-4-ylboronic acid (**4**), 4-(4,4,5,5-tetramethyl-1,3,2-dioxaborolan-2-yl)phenol (**5**) and 9,9-dioctylfluoren-2,7-yl-bis(trimetilen)borate (**6**) were purchased from Aldrich.

General procedure for the Suzuki coupling[30]. The reaction was conducted under argon using Schlenk techniques and dry solvents, toluene or dimethoxyethane. Tetrakis(triphenylphosphine)palladium(0) [$Pd(PPh_3)_4$] was purchased from Aldrich and used as received. The experimental details for the synthesis of 2,7′-bis(4-cyanophenyl)-9,9,9′,9′-tetra(*n*-octyl)-2′,7-bifluorene **CN-PFFP-CN**, are given as an example.

A Schlenk tube was charged with $Pd(PPh_3)_4$ (0.05 mmol, 5% mol the amount of the boronic acid) and 2,7′-dibromo-9,9,9′,9′-tetra(*n*-octyl)bifluorene (**2**) (0.44 mmol) and purged by several vacuum–argon cycles. Dimethoxyethane (3 mL) was added *via* syringe and the mixture stirred at 75 °C for 30 min. Then, 4-cyanophenylboronic acid (**3**) (0.92 mmol) dissolved in dimethoxyethane (3 mL) and 2 M Na_2CO_3 (2.3 mL, a five-fold molar amount with respect to the boronic acid) was added also *via* syringe. The reaction was stirred at 75 °C for 32 h. After cooling at room temperature, the

reaction crude was filtered through a pad of Celite® and the brownish solution diluted with water (3 mL). The aqueous solution was extracted with ethyl acetate; the combined organic layers were washed with water, dried over anhydrous $MgSO_4$ and evaporated to dryness. The isolated yellow oil was purified by medium-pressure chromatography on silica gel using hexane as eluant and gradually increasing the polarity with dichloromethane. The desired compound **CN-PFFP-CN** was obtained as a white solid (0.16 g, 37% yield).

CN-PFFP-CN: ν_{max} (KBr) cm^{-1} 2224 (CN); 1602, 1509 (Ar, C–C); 813 (Ar); δ_H (400 MHz; $CDCl_3$) 7.86–7.81 (m, 4H), 7.80 (d, J = 8.7 Hz, 4H), 7,77 (d, J = 8.7 Hz, 4H), 7.74–7.69 (m, 2H), 7.68–7,66 (m, 2H), 7.64–7.58 (m, 4H), 2.17–2.06 (m, 8H), 1.24–1.04 (m, 40H), 0.85–0.72 (m, 20H); δ_C(100 MHz; $CDCl_3$) 152.00, 151.84, 146.03, 141.44, 140.83, 139.52, 137.81, 132.53, 127.66, 126.29, 126.26, 121.48, 121.43, 120.28, 119.04, 110.51, 55.39, 40.27, 31.71, 31.38, 30.13, 29.12, 23.78, 22.53, 14.00; Found: C, 87.48; H, 9.33; N, 2.70%. Calc. for $C_{72}H_{88}N_2$: C, 88.11; H, 9.04; N, 2.85%; m/z (MALDI-TOF, dithranol) 980.6 $[M]^+$, calc. 980.69.

Synthesis of 2,7′-Bis(4′-cyanobiphenyl)-9,9,9′,9′-tetra(*n*-octyl)-2′,7-bifluorene CN-PPFFPP-CN. The compound was obtained from the dibromide (**2**) and boronic acid (**4**), and purified following the described general procedure for Suzuki coupling (23% yield).

CN-PPFFPP-CN: ν_{max} (KBr) cm^{-1} 2226 (CN); 1604, 1461 (Ar, C–C), 814 (Ar); δ_H (400 MHz; $CDCl_3$) 7.86–7.80 (m 8H), 7.79–7.75 (m, 8H), 7.74–7.66 (m, 8H), 7.66–7.62 (m, 4H), 2.18–2.02 (m, 8H), 1.21–1.03 (m, 40H), 0.85–0.71 (m, 20H), δ_C (100 MHz; $CDCl_3$) 151.82, 151.75, 145.24, 142.02, 140.67, 140.60, 139.88, 138.97, 137.87, 132.70, 127.82, 127.61, 127.51, 126.20, 126.00, 121.44, 121.35, 120.19, 120.15, 119.02, 110.84, 55.35, 40.46, 31.81, 30.03, 29.27, 29.23, 23.80, 22.65, 14.10; Found: C, 88.32; H, 8.94; N, 2.17%. Calc. for $C_{84}H_{96}N_2$: 88.99; H, 8.54; N, 2.47%; m/z (MALDI-TOF, dithranol) 1132.8 $[M]^+$, calc. 1132.76.

Synthesis of CN-PFP-CN and the intermediate CN-PFP-Br. The reaction was conducted adapting the described general procedure for Suzuki coupling. The title compounds were prepared by reacting the dibromide (**1**) and the boronic acid (**3**) in 1 : 1.05 molar ratio using dimethoxyethane as reaction media. **CN-PFP-CN** (35% yield) and **CN-PF-Br** (25% yield) were separated by medium-pressure chromatography on silica gel using hexane as eluant and gradually increasing the polarity with dichloromethane.

CN-PFP-CN: ν_{max} (KBr) cm^{-1} 2226 (CN); 1604, 1465 (Ar, C–C), 812 (Ar); δ_H (400 MHz; $CDCl_3$) 7.83 (d, J = 7.9 Hz, 2H), 7.76 (s, 8H), 7.61 (dd, J_1 = 7.9 Hz, J_2 = 1.5 Hz, 2H) 7.56 (d, J = 1.5 Hz, 2H), 2.09–2.01 (m, 4H), 1.20–1.01 (m, 20H), 0.78 (t, J = 7.0, 6H), 0.73–0.64 (m, 4H); δ_C (100 MHz; $CDCl_3$) 152.10, 145.92, 140.92, 138.45, 132.64, 127.77, 126.48, 121.69, 120.65, 119.05, 110.70, 55.50, 40.32, 31.72, 29.93, 29.14, 29.14, 23.85, 22.67, 14.09; Found: C, 87.35; H, 8.40; N, 4.70%. Calc. for $C_{43}H_{48}N_2$: C, 87.11; H, 8.16; N, 4.73%;. m/z (MALDI-TOF, dithranol) 592.3 $[M]^+$, calc. 592.38.

CN-PF-Br: ν_{max} (KBr) cm^{-1} 2224 (CN); 1605, 1456 (Ar, C–C); 814 (Ar); δ_H (400 MHz; $CDCl_3$) 7.78–7.72 (m 5H), 7.61–7.55 (m, 2H), 7.53–7.46 (m, 3H), 2.05–1.90 (m, 4H), 1.23–0.98 (m, 20H), 0.80 (t, J = 7.1 Hz, 6H), 0.68–0.55 (m, 4H); δ_C (100 MHz; $CDCl_3$) 153.20, 151.45, 145.95, 140.76, 139.27, 183.35, 132.67, 130.16, 127.76, 126.48, 126.29, 121.62, 121.42, 121.45, 120.35, 119.03, 110.74, 55.69, 40.26, 31.75, 29.96, 29.26, 29.15, 23.77, 22.65, 14.1.0.

Synthesis of 2,7′′-bis(4-cyanophenyl)-9,9,9′,9′,9′′,9′′-hexa-(*n*-octyl)-2′,2′′,7,7′′-terfluorene CN-PFFFP-CN. The title compound was obtained from the bromide **CN-PF-Br** and the diboronate (**6**) in a 2.04 : 1 molar ratio using toluene as the reaction medium. The compound was purified by medium-pressure chromatography on silica gel using hexane as eluant and gradually increasing the polarity with dichloromethane (56% yield).

CN-PFFFP-CN: ν_{max} (KBr) cm^{-1} 2227 (CN); 1604, 1460 (Ar, C–C) 813 (Ar); δ_H (400 MHz; $CDCl_3$) 7.87–7.81 (m, 6H), 7.79 (d J = 8.8 Hz, 4H), 7.76 (d, J = 8.8 Hz, 4H), 7.73–7.64 (m, 8H), 7.63–7.56 (m, 4H), 2.18–2.01 (m, 12H), 1.23–1.01 (m, 60H), 0.87–0.68 (m, 30H); δ_C (100 MHz; $CDCl_3$) 152.03, 151.84, 151.81, 146.12, 141.50, 141.08, 140.36, 140.17, 139.40, 137.85, 132.66, 127.74, 126.31, 126.28, 126.29, 121.50, 121.41, 120.34, 120.22, 120.04, 119.11, 110.57, 55.45, 55.38, 40.32, 40.21, 31.87, 31.76, 30.03, 29.97, 29.95, 29.26, 29.14, 23.91, 23.82, 23.78, 22.68, 22.54, 14.08, 14.02; Found: C, 88.44; H, 9.56; N, 2.11%. Calc. for $C_{101}H_{128}N_2$: C, 88.54; H, 9.42; N, 2.04%; m/z (MALDI-TOF, dithranol) 1370.1 $[M+H]^+$, calc. 1369.01.

Synthesis of 4,4′-(9,9,9′,9′-tetrakis(*n*-octyl)bifluorenyl-7-yl)-diphenol HO-PFFP-OH. This intermediate was prepared following the described general procedure for Suzuki coupling from dibromide (**2**) and boronate (**5**) in 1 : 2.10 molar ratio at 90 °C using toluene as the reaction media. Purification was afforded by flash column chromatography on silica gel using hexane–ethyl acetate 10 : 1 as eluant (35% yield).

HO-PFFP-OH: ν_{max} (KBr) cm^{-1} 3424–3379 (OH); 1604, 1518 (Ar, C–C); 1258, 1201, 1060 (C–O); 812 (Ar); δ_H (400 MHz; $CDCl_3$) 7.77–7.52 (m, 10H), 7.02 (dd, J_1 = 7.5 Hz, J_2 = 1.7 Hz, 2H), 6.96 (dd, J_1 = 7.5 Hz, J_2 = 1.7 Hz, 2H), 2.10–2.05 (m, 4H), 1.23–1.11 (m, 20H), 0.84 (t, J = 6.9 Hz, 6H), 0.80–0.77 (m, 4H); δ_C (100 MHz; $CDCl_3$) 155.11, 151.67, 139.65, 139.57, 134.49, 128.47, 125.62, 121.09, 119.94, 115.83, 55.26, 40.52, 31.84, 30.09, 29.27, 29.23, 23.88, 22.65, 14.14.

Synthesis of 2,7′-di(4(4(4-pentylphenyl)benzoyloxy)phenyl)-9,9,9′,9′-tetrakis(n-octyl)-2′,7-bifluorene C_5PPCOO-PFFP-OCOPPC_5. The compound **HO-PFFP-OH** (0.19 mmol, 0.18 g) and distilled triethylamine (0.68 mmol, 100 μL) were dissolved in dried dichloromethane (6 ml) under argon atmosphere. The acid chloride 4-(4-pentylphenyl)benzoyl chloride (**7**) (0.45 mmol, 0.13 g) dissolved in the minimum amount of dichloromethane was added and the reaction stirred at room temperature for 4 h. The precipitate was filtered off and the solvent removed under vacuum. The crude was purified by medium-pressure chromatography on silica gel

using hexane as eluant and gradually increasing the polarity with ethyl acetate to provide the title compound (58% yield).

C_5PPCOO-PFFP-OCOPPC_5: ν_{max} (KBr) cm^{-1} 1736 (C=O); 1606, 1461 (Ar, C–C); 1263 (C–O); 806 (Ar); δ_H (400 MHz; $CDCl_3$) 8.30 (d, J = 8.0 Hz, 4H), 7.82 (d, J = 7.7 Hz, 4H) 7.78–7.71 (m, 8H), 7.71–7.57 (m, 12H), 7.35 (d, J = 8.3 Hz, 4H), 7.32 (d, J = 7.9 Hz, 4H), 2.68 (t, J = 7.7 Hz, 4H), 2.15–2.04 (m, 8H), 1.68 (q, J = 6.9 Hz, 4H), 1.42–1.32 (m, 8H), 1.22–1.05 (m, 44H), 0.92 (t, J = 6.2 Hz, 18H), 0.85–0.73 (m, 8H); δ_C (100 MHz; $CDCl_3$) 165.20, 151.84, 151.75, 150.30, 146.31, 143.46, 140.58, 140.25, 139.99, 139.52, 139.24, 137.14, 130.76, 129.11, 128.25, 127.98, 127.27, 127.03, 126.13, 126.04, 122.07, 121.60, 121.42, 120.08, 120.00, 55.36, 40.47, 35.62, 31.85, 31.53, 31.21, 30.09, 29.28, 29.24, 23.92, 22.60, 22.61, 14.17, 14.02; Found: C, 85.98; H, 8.96%. Calc. for $C_{106}H_{126}O_4$: C, 86.95; H, 8.67%; m/z (MALDI-TOF, dithranol) 1464.0 $[M+H]^+$, calc. 1462.97.

Instrumentation

Infrared spectra were measured on an ATI-Matsson Genesis Series FTIR from either nujol mulls between KBr pellets. ^{1}H NMR and ^{13}C NMR spectra were recorded on a Bruker AV-400 operating at 400 or 100 MHz. Elemental analysis was performed with a Perkin-Elmer 240C microanalyzer. Matrix-assisted laser desorption ionization-time-of-flight mass spectrometry (MALDI-TOF-TOF) was performed at the Sidi Service of the Universidad Autónoma (Madrid) on a 4700 Proteomic analyzer from Applied Biosystems using dithranol as the matrix.

The optical textures of the mesophases were studied with an Olympus BH-2 polarizing microscope equipped with a Linkam THMS600 hot stage and a CS196 cooling system. Differential scanning calorimetry (DSC) was performed using a DSC Q2000 from TA Instruments with samples ($\sim$3 mg) sealed in aluminium pans at a scanning rate of 10 or 20 °C min^{-1} under a nitrogen atmosphere. Temperatures were read at the maximum of the transition peaks, and the glass transition temperature was read at the midpoint of the heat capacity increase. Thermogravimetric analysis (TGA) was performed at 10 °C/min under nitrogen atmosphere using a TGA Q5000IR from TA Instruments. TGA data are given as the onset of the decomposition curve, and DTGA data is given at the maxima of the weight derivative curve peaks.

UV-vis absorption spectra were measured with a UV4-200 from ATI-Unicam using 10^{-4}–10^{-5} M solutions in THF. Fluorescence spectra were measured with a Perkin-Elmer LS50B spectrofluorimeter using solutions in THF of *ca.* 0.01 absorbance (about 10^{-6}–10^{-7} M) under excitation at the absorption maximum. Emission quantum yields (ϕ_{em}) were measured relative to 9,10-diphenylanthracene (ϕ_{em} = 0.90 in cyclohexane)[36] from corrected emission spectra.

Cyclic voltammetry experiments in dichloromethane solutions (10^{-3} M) containing tetrabutylammonium hexafluorophosphate (0.1 M) as the supporting electrolyte were performed using an EcoChemie Instrument. A three-electrode cell was used where the working electrode was a graphite electrode, a platinum wire was used as counter electrode and an Ag/AgCl electrode was used as a reference. The solutions were purged with argon. Cyclic voltammograms were obtained at room temperature with scan rates of 100 mV/s.

Preparation of linearly polarized photoluminescent films

Films of oligofluorenes in a nematic matrix were prepared by *in situ* photopolymerisation of reactive liquid-crystalline blends.[25–27,37] Reactive mixtures consisted of a non-emissive liquid-crystalline matrix and a 5% molar ratio of the fluorene-based emissive guest. The liquid-crystalline matrix was composed of 85% molar ratio of 1,2-di[4-(6-acryloyloxyhexyloxy)-benzoyloxy]-2-methylbenzene (C6M) and 10% molar ratio of 1-[4-(6-acryloyloxyhexyloxy)benzoyloxy]-2-methyl-4-(4-octyl-benzoyloxy)benzene (C6Mm). C6M is a difunctional liquid-crystalline monomer that causes cross-linking in the final polymeric system; it has a nematic phase in the range 86–116 °C and shows a maximum absorbance at 268 nm (in THF). C6Mm is a monofunctional liquid-crystalline monomer that has a nematic phase between 53 and 136 °C and a maximum absorbance at 265 nm (in THF). The photo-polymerizable mixtures were prepared by dissolving C6M (10% molar), C6Mm (85% molar), the oligofluorene (5% molar), 1% (w/w) of the photoinitiator Irgacure 784-DC (a blend of 30% bis(η^5-2,4-cyclopentadien-1-yl)-bis[2,6-difluoro-3-(1*H*-pyrrol-1-yl)phenyl]titanium with 70% Dicalite) and 200 ppm of the thermal inhibitor 2,6-di-*tert*-butyl-4-methylphenol in freshly distilled dichloromethane. The solvent was evaporated at room temperature and residual solvent was removed under vacuum. During their preparation, storage and handling, the samples were suitably protected and kept away from light. The thermal properties of the reactive mixtures were determined by DSC and POM; they present a nematic phase between 60 and 125 °C.

Light-induced photopolymerization was carried out by irradiation of the molten reactive sample with an OSRAM Ultravitalux 300 W lamp using both a 400 nm long-pass filter and an IR filter between the lamp and the sample. Irradiation was maintained for 10 min.

Photopolymerization of the reactive mixtures was investigated by photo-DSC using a Perkin–Elmer DSC-7 suitably modified for light irradiation. The sample (2–4 mg) was placed in an open aluminium pan and the experiment was carried out under a nitrogen atmosphere to avoid oxygen inhibition. The light source was at a distance of 30 cm from the sample and the reference holders. The polymerization conversion was calculated of approx. 75% from the enthalpy content of the polymerization peak recorded on the DSC. Reference value was 78 kJ/mol as the polymerization enthalpy of an acrylate group.

Films were produced by irradiation of the molten sample inside a commercial LC cell (Linkam 5 μm) in a thermostatic stage at a controlled temperature. The reactive mixture was introduced by capillary action at the mesophase temperature (80–100 °C) and cooled down to the polymerization temperature (60 °C). The irradiation source was located 20 cm from the cell.

Fabrication of the electroluminescence devices and measurements

EL devices were prepared by using a configuration ITO/PEDOT:PSS/oligofluorene:PS/Ba/Ag. Devices were constructed

by spin-coating a 100 nm layer of PEDOT:PSS onto an indium–tin oxide (ITO) coated glass to aid the injection of holes and to increase the device preparation yield. Then, a 100 nm emitting layer consisting of a 50 wt% blend of the oligofluorene and polystyrene (PS) was also deposited by spin-coating from a toluene solution. The thickness of the films was determined using an Ambios XP1 profilometer. Finally, a barium cathode (5 nm) capped with a silver layer (60 nm) was thermally evaporated using a shadow mask under vacuum ($<1 \times 10^{-6}$ mbar) using an Edwards Auto500 evaporator. The metal evaporator is integrated into an inert atmosphere glovebox (<0.1 ppm O_2 and H_2O).

To obtain good quality films, the emitting layer was composed of 50 wt% of the corresponding oligofluorene in PS (from Aldrich, M_n = 140 000, PI = 1.6). This composition was selected after studying the EL properties of blends having different compositions (from 25 to 80 wt% of oligofluorene).

Current density and luminance *versus* voltage were measured using a Keithley 2400 source meter and a photodiode coupled to a Keithley 6485 pico-amperometer using a Minolta LS100 camera to calibrate the photocurrent. External quantum efficiencies (EQEs) were determined using an integrated sphere coupled to an UDT instruments S370 Optometer. An Avantes luminance spectrometer was used to measure the EL spectrum. Characterization was performed in an inert atmosphere glovebox (<0.1 ppm O_2 and H_2O, M. Braun).

Conclusions

In this paper we report the synthesis, characterization and mesomorphic behavior of a series of novel fluorene-based luminophores whose common structural feature is a short oligofluorene central core extended at its ends with a pro-mesogenic unit. The analysis of the presented structures shows that the elongation of a bifluorene-based core with 4′-cyanobiphenyl or phenyl 4′-pentylbiphenyl-4-carboxylate pro-mesogenic groups is an adequate strategy to promote liquid-crystallinity. In this sense, the presented compounds having a molecular core with a small number of aromatic rings represent an approach better than the systematic elongation of the aromatic core by fluorene units in order to minimize the synthetic complexity. Also, this strategy is satisfactory to tune the optical properties, providing efficient emitters in the violet–blue region of the electromagnetic spectra, in particular when electro-withdrawing cyano end-groups are found at the end or the emitting core. However, the presence of ester groups within the core is not as favorable regarding the optical properties.

The compounds with electron-withdrawing nitrile groups were synthesized to study the effect of the substituents on the electrochemical properties of these oligomers. The described compounds have lower LUMO, *i.e.* better electron affinity, than related oligofluorenes. Preliminary results demonstrate that electroluminescence can be observed from simple solution-processed OLEDs using these oligomers as the only optically and electrically active species.

All these extended molecules spontaneously align within a nematic matrix to produce polarized emitting films by *in situ* photopolymerization. From all the investigated compounds, the liquid-crystalline **CN-PPFFPP-CN** and **C_5PPCOO-PFFP-OCOPPC_5** are the most suitable luminophores as they combine a set of structural features compatible with the formation of mesophases and appropriate emissive properties. Optical anisotropic films with emission polarization values of 8 have been processed. These values are comparable to those previously reported for shorter one-fluorene-based emitters with a PFFPCN core[25] where the fluorene is covalently bonded by an hexyloxy spacer to an oriented network processed under the same conditions, provided that is easier to synthesize structurally symmetric compounds and taken into account that the increase on the number of alkyl chains limits the emission anisotropy. It is worth mentioning that a larger emission polarization has been reported for a related fluorene without side-alkyl chains to the detriment of the photostability of the films.

Acknowledgements

The Universidad de Zaragoza acknowledges financial support from MEC-FEDER Spanish project MAT2008-06522-C02-01 and from the Departamento de Ciencia, Tecnología y Universidad of the Government of Aragón and FEDER founding. J. del Barrio acknowledges his grant from the Government of Aragón.

References and notes

1 A. C. Grimsdale, K. L. Chan, R. E. Martin, P. G. Jokisz and A. B. Holmes, *Chem. Rev.*, 2009, **109**, 897.
2 A. C. Grimsdale and K. Müllen, *Macromol. Rapid Commun.*, 2007, **28**, 1676.
3 U. Scherf and E. J. W. List, *Adv. Mater.*, 2002, **14**, 477.
4 D. Neher, *Macromol. Rapid Commun.*, 2001, **22**, 1365.
5 M. Leclerc, *J. Polym. Sci., Part A: Polym. Chem.*, 2001, **39**, 2867.
6 Y. Geng, S. W. Culligan, A. Trajkovska, J. U. Wallace and S. H. Chen, *Chem. Mater.*, 2003, **15**, 542.
7 Y. Geng, A. Trajkovska, D. Katsis, J. J. Ou and S. W. Culligan, *J. Am. Chem. Soc.*, 2002, **124**, 8337.
8 J. Jo, C. Chi, S. Höger, G. Wegner and D. Y. Yoon, *Chem.–Eur. J.*, 2004, **10**, 2681.
9 R. E. Martin and F. Diederich, *Angew. Chem., Int. Ed.*, 1999, **38**, 1350.
10 S.-H. Yang and C. S. Hsu, *J. Polym. Sci., Part A: Polym. Chem.*, 2009, **47**, 2713.
11 M. Grell, W. Knoll, D. Lupo, A. Meisel, T. Miteva, D. Neher, H. G. Nothofer, U. Scherf and A. Yasuda, *Adv. Mater.*, 1999, **11**, 671.
12 K. S. Whitehead, M. Grell, D. D. C. Bradley, M. Jandke and P. Strohriegl, *Appl. Phys. Lett.*, 2000, **76**, 2946.
13 D. Sainova, A. Zen, H. G. Nothofer, U. Asawapirom, U. Scherf, R. Hagen, T. Bieringer, S. Kostromine and D. Neher, *Adv. Funct. Mater.*, 2002, **12**, 49.
14 S. W. Culligan, Y. Geng, S. H. Chen, K. Klubek, K. M. Vaeth and C. W. Tang, *Adv. Mater.*, 2003, **15**, 1176.
15 K. L. Woon, M. P. Aldred, P. Vlachos, G. H. Mehl, T. Stirner, S. M. Kelly and M. O'Neill, *Chem. Mater.*, 2006, **18**, 2313.
16 K. L. Woon, A. E. Contoret, S. R. Farrar, A. Liedtke, M. O'Neill, P. Vlachos, M. P. Aldred and S. M. Kelly, *J. Soc. Inf. Disp.*, 2006, **16**, 557.
17 M. P. Aldred, P. Vlachos, A. E. A. Contoret, S. R. Farrar, W. Chung-Tsoi, B. Moonsor, K. L. Woon, R. Hudson, S. M. Kelly and M. O'Neill, *J. Mater. Chem.*, 2005, **15**, 3208.
18 M.-C. Choi, Y. Kim and C.-S. Ha, *Prog. Polym. Sci.*, 2008, **33**, 581.

19 M. P. Aldred, A. J. Eastwood, S. M. Kelly, P. Vlachos, A. E. A. Contoret, S. R. Farrar, B. Mansoor, M. O'Neill and W. C. Tsoi, *Chem. Mater*., 2004, **16**, 4928.
20 H. Thiem, M. Jandke, D. Hanft and P. Strohriegl, *Macromol. Chem. Phys*., 2006, **207**, 370.
21 H. P. Rathnayake, A. Cirpan, Z. Delen, P. M. Lahti and F. E. Karasz, *Adv. Funct. Mater*., 2007, **17**, 115.
22 G. W. Gray and A. Ibbotson, *J. Chem. Soc*., 1957, 3228.
23 I. R. Davison, D. M. Hall and I. Sage, *Mol. Cryst. Liq. Cryst*., 1985, **129**, 17.
24 F. H. Boardman, D. A. Dunmur, M. C. Grossel and G. R. Luckhurst, *Chem. Lett*., 2002, 60.
25 M. Millaruelo, L. S. Chinellato, J. L. Serrano, L. Oriol and M. Pinol, *J. Polym. Sci., Part A: Polym. Chem*., 2007, **45**, 4804.
26 M. Millaruelo, L. Oriol, J. L. Serrano, M. Piñol and P. L. Saez, *Mol. Cryst. Liq. Cryst*., 2004, **411**, 1493.
27 M. Millaruelo, L. Oriol, M. Piñol, P. L. Saez and J. L. Serrano, *J. Photochem. Photobiol., A*, 2003, **155**, 29.
28 M. P. Aldred, A. J. Eastwood, S. P. Kitney, G. J. Richards, P. Vlachos, S. M. Kelly and M. O'Neill, *Liq. Cryst*., 2005, **32**, 1251.
29 Y. Lin, Z.-K. Chen, T.-L. Ye, Y.-F. Dai, D.-G. Ma, Z. Ma, Q. D. Liu and Y. Chen, *Polymer*, 2010, **51**, 1270.
30 L. S. Chinelatto, J. del Barrio, M. Piñol, L. Oriol, M. A. Matranga, M. P. De Santo and R. Barberi, *J. Photochem. Photobiol., A*, 2010, **210**, 130.
31 C. Chi and G. Wegner, *Macromol. Rapid Commun*., 2005, **26**, 1532.
32 X. Zhan, S. Wang, Y. Liu, X. Wu and D. Zhu, *Chem. Mater*., 2003, **15**, 1963.
33 We have reported the synthesis and characterization of these oligofluorenes in ref. 30. We have estimated for the corresponding difluorene, trifluorene and tetrafluorene the following values for the HOMO: −5.65, −5.53, −5.53 eV; and for the LUMO: −2.23, −2.35, −2.43 eV. These values are in close agreement with those determined by electrochemical measurements reported by Chi *et al*. in ref. 31.
34 A. K. Mishra, M. Graf, F. Grasse, J. Jacob, E. J. W. List and K. Müllen, *Chem. Mater*., 2006, **18**, 2879.
35 P. K. Tsolakis and J. K. Kallitsis, *Chem.–Eur. J*., 2003, **9**, 936.
36 D. Eaton, *Pure Appl. Chem*., 1988, **60**, 1107.
37 R. Gimenez, L. Oriol, M. Pinol, J. L. Serrano, A. I. Vinuales, T. Fisher and J. Stumpe, *Helv. Chim. Acta*, 2006, **89**, 304.